M. Uzielli · F. Catani · V. Tofani · N. Casagli

Risk analysis for the Ancona landslide—II: estimation of risk to buildings

Abstract This paper illustrates the quantitative estimation of specific risk (i.e., the product of hazard and vulnerability) for 39 buildings located upon the Ancona landslide based on the characterization of landslide kinematics presented in a companion paper. Hazard is quantified based on intensity, intended as the damaging potential of the kinetic and/or geometric attributes of the landslide, and is expressed in terms of expected exceedance of preset cumulative displacement thresholds for a set of five reference time intervals, ranging from 1 to 100 years. The estimation of hazard relies sequentially on (1) Monte Carlo simulation of displacement series, with sampling distributions of average yearly displacement defined on the basis of the statistical processing of inclinometer and radar interferometer data; and (2) the subsequent spatialization of displacement using radial basis interpolation as described in the companion paper. The vulnerability of the set of buildings relies on a quantitative model in which vulnerability is a function of landslide intensity and the resilience of the buildings. Resilience is a function of a set of indicators including structural type, age, and foundation type and is temporally variable due to the progressive structural degradation. Hazard, vulnerability, and specific risk are estimated for the set of five aforementioned reference time intervals. The magnitude and temporal dependence of hazard, vulnerability, and specific risk are assessed critically.

Keywords Ancona landslide · Intensity · Hazard · Vulnerability · Risk

Introduction

Reference risk model

Ideally, quantitative risk estimation (QRE) is preferred to a qualitative estimation for natural hazards as it allows for a rigorous and systematic assessment and an improved basis for communication between the various categories involved in technical and political decision-making. Examples of QRE for landslides are available in the technical literature, e.g., Dai et al. (2002), Catani et al. (2005), Glade et al. (2005), Hungr et al. (2005), Sassa and Canuti (2008), Zêzere et al. (2008), Ho and Ko (2009), Jaiswal et al. (2010, 2011), and Lee and Jones (2013). The considerable heterogeneity in conceptual approaches to risk estimation is a well-known fact. No univocal quantitative definition for risk is available at present, and the conceptual unification of risk analysis methods currently appears to be a practically unattainable goal. A consistent quantitative risk estimation analysis must rely on a reference risk framework. UNDRO (1979), for instance, proposed the following model, which is widely adopted in the geohazards community, and in which risk is calculated as the product of three macro-factors:

$$R = H \cdot V \cdot E \qquad (1)$$

where R=risk; H=hazard; V=vulnerability, and E=value of elements at risk. To avoid the undesirable consequences of misinterpretations

of risk estimates and assessment due to the aforementioned terminological fragmentation, it is essential to provide reference definitions explicitly. In the ISSMGE TC304 "Engineering Practice of Risk Assessment and Management" Glossary (ISSMGE 2004), hazard is "the probability that a specific hazardous event occurs within a given period of time"; vulnerability is defined as "the degree of expected loss (from 0: no loss expected; to 1: total loss expected) in an element or system in relation to a specific hazardous event", while the "elements at risk" macro-component parameterizes the value of vulnerable physical or nonphysical assets in a reference system. Consequently, risk can be defined as "the probability of the manifestation of a given level of loss in physical or non-physical assets within a given time period as the result of the occurrence of a specific hazardous event". The measurement units of elements at risk are not univocal and depend on the typology of elements at risk. The value of physical assets, for instance, is usually measured and expressed in financial units, while the value of lives has been parameterized in the risk analysis literature using both financial and nonfinancial units (e.g. "equivalent fatalities"). The reference risk equation can be rewritten as

$$R = R_s \cdot E \qquad (2)$$

in which

$$R_s = H \cdot V \qquad (3)$$

is the specific risk, i.e., the probability of adverse degree of loss related to a hazardous event of a given magnitude.

The objective of this paper is the quantitative estimation of specific risk for a set of 39 buildings located inside the Ancona landslide area. Any quantitative estimation effort entails the acceptance of uncertainties. Among other georisks, landslide risk ranks among the most complex to estimate confidently (e.g., Li et al. 2010; Lee and Jones 2013). The inherent complexity of landslide phenomena and the invariably limited and "insufficient" quantity of monitoring data result in the existence of considerable uncertainty in quantitative estimates. In the present case, uncertainties in specific risk estimates stem from uncertainties in both hazard and vulnerability. Uncertainty in hazard is due mainly, but not solely, to (a) limited number and size of monitoring data samples (inclinometer and interferometer data) and (b) the uncertainty in displacement statistics at building locations, stemming from the imperfect spatial interpolations. Uncertainties in vulnerability stem at least from (a) subjectivity and vagueness in damage survey data, (b) uncertainty in resilience model and submodels, and (c) uncertainty and subjectivity in the empirical intensity model. Here, emphasis is placed on the illustration and implementation of a structured, quantitative procedure that may be as conceptually rigorous—and practically meaningful—as possible. It is worth to remark that QRE does not necessarily produce a more accurate or better result than qualitative assessment; however, it

relies on the rigorous assessment of conceptual models and on a systematic analysis of implicit uncertainty. Though there is considerable space and need for refinement of quantitative estimation procedures as the one proposed herein, their application to case studies is paramount for their progressive improvement.

Vulnerability model

The importance of assessing vulnerability is increasingly recognized by the georisk community. Large-scale international research efforts such as the European Community FP6 LESSLOSS (www.lessloss.org) and the FP7 MOVE (www.move-fp7.eu) and Safeland (www.safeland-fp7.eu) projects have focused on the quantification of vulnerability from a technical perspective. A comprehensive conceptual outlook on the topic of technical vulnerability estimation is given in Birkmann (2006). Methods for the estimation of vulnerability to landslides for specific categories of vulnerable elements (e.g., Mavrouli and Corominas (2010) for simple reinforced concrete buildings) or for specific landslide types (e.g., Mansour et al. (2011) for slow-moving landslides) have been proposed recently. However, the range of more general methods for quantitative estimation of vulnerability to landslides is still relatively limited.

Uzielli et al. (2008) proposed a quantitative model in which vulnerability was given by the product of landslide intensity and the susceptibility of vulnerable elements to suffer damage. Quantitative analytical model structures were proposed for intensity and susceptibility; the concepts of intensity factors and susceptibility factors were introduced to enable the quantitative parameterization of landslide attributes and vulnerability indicators. Li et al. (2010) expressed vulnerability as a more complex function of intensity and the resistance of vulnerable elements to hazardous events. Both contributions highlighted the fact that all analytical models were to be regarded as initial proposal for a quantitative approach to vulnerability estimation, requiring progressive refinement and calibration through, for instance, application to case studies (see, e.g., Kaynia et al. 2008), new research efforts, and more dedicated collection and processing of survey data.

Here, the analytical structure of the vulnerability model given in Li et al. (2010) is preserved, but resistance is replaced by the resilience index. The latter is deemed conceptually and semantically more adequate as it refers to the inherent capability of vulnerable assets to preserve integrity, functionality, and desired performance in the course of the interaction with a reference hazardous event. Moreover, from an operational point of view, the models for intensity and resistance proposed by Li et al. (2010) were not constrained to yield a common range of values, thereby making the appreciation of the relative magnitude of the two vulnerability factors less intuitive. Vulnerability is thus given by:

$$V = \begin{cases} \dfrac{2I^2}{\Omega^2} & \dfrac{I}{\Omega} < 0.5 \\ 1.0 - \dfrac{2(\Omega - I)^2}{\Omega^2} & 0.5 \leq \dfrac{I}{\Omega} \leq 1.0 \\ 1.0 & \dfrac{I}{\Omega} > 1.0 \end{cases} \quad (4)$$

in which I is the intensity parameter and Ω is the resilience index. This paper refers to intensity and resilience models which are defined in the range [0, 1] as detailed in the following. Figure 1 plots the vulnerability curves calculated using Eq. (4) for several values of the resilience parameter Ω.
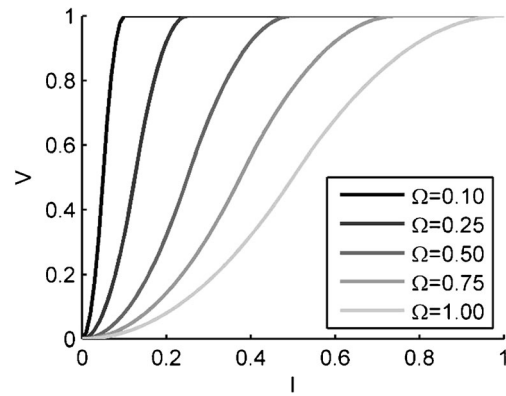

Fig. 1 Intensity-vulnerability functions for selected discrete values of resilience

Parameterization of landslide intensity

Landslide intensity parameterizes the damaging potential of a landslide through its kinetic and/or geometric attributes. The formulation of a quantitative, empirical intensity model entails the definition of a dependent variable (intensity) with one or more independent variables serving as intensity factors. No univocal set of intensity factors, representative of the kinetic and geometric attributes, is available to estimate intensity, though a variety of these have been used in previous studies (see, e.g., Hungr 1997; Amatruda et al. 2004; Uzielli et al. 2008; Li et al. 2010). Uzielli et al. (2008) introduced the concept of kinetic and kinematic intensity factors, as well as general models for their calculation and for the terminal calculation of intensity based on these.

For the purpose of the present case study, as the Ancona landslide is a slow landslide (e.g., Agostini et al. 2014), it is suitable to define an intensity parameter in terms of ground displacement (geometric attribute) rather than velocity (kinetic attribute).

The parameterization of landslide intensity for the purpose or risk estimation is structured as follows: (1) definition of a posterior intensity model; (2) posterior estimation of vulnerability of buildings from the 13 December 1982 event; (3) quantitative estimation of building resilience during the 13 December 1982 event; (4) back-calculation of intensity for the 13 December 1982 event; and (5) formulation of an analytical intensity model from back-calculated intensity and estimated kinematic factors (i.e., ground displacements) as given in Uzielli et al. (2014). The above procedure is detailed sequentially in the forthcoming sections.

Definition of posterior intensity

The expression for posterior (i.e., back-calculated) intensity at the location of any building is calculated from the reference vulnerability model given in Eq. (4):

$$I_P = \begin{cases} \Omega \sqrt{\dfrac{V_P}{2}} & \text{for } V_P \leq 0.50 \\ \Omega \left(1 - \dfrac{\sqrt{2 - 2V_P}}{2}\right) & \text{for } V_P > 0.50 \end{cases} \quad (5)$$

in which I_P is the posterior landslide intensity, V_P is the posterior vulnerability, and Ω is the resilience of vulnerable elements. It should be noted that the "posterior" refers specifically to the 13 December 1982 event for which post-event survey data are available.

Estimation of posterior vulnerability

Posterior vulnerability, or "observed degree of loss" was back-estimated from available post-event survey data compiled by the Ancona municipality (Comune di Ancona) following the 13 December 1982 event on 70 buildings located inside the landslide perimeter, of which 60 still exist and 10 were demolished in the following years (Comune di Ancona 1985). Figure 2a shows the location and the present state (existing/non existing) of the buildings. A set of three typological attributes (structural typology, age of building, foundation type) and seven damage categories were selected as relevant indicators for the quantitative estimation of posterior vulnerability. The damage indicators expressed the damage observed to: (1) main structures; (2) floors; (3) perimetral walls; (4) internal walls; (5) internal stairs; (6) external stairs; and (7) retaining structures. Panels b–d of Fig. 2 illustrate the categorization of buildings by structural typology, age, and foundation type, respectively, as given in the post-landslide survey. Figures 3 and 4 plot the observed damage to the set of 70 surveyed buildings as assessed in the survey. The damage indicators for the main structures (D-MS), floors (D-FL), perimeter walls (D-PW), internal walls (D-IW), and internal staircases (D-IS), defined by the notation G_k, are expressed on a scale from 1 (no damage) to 5 (complete destruction). The damage indicators for external staircases (D-ES) and retaining walls (D-RW) are expressed on a binary scale (0: no damage; 1: damage).

The reference model for posterior vulnerability is

$$V_p = \sum_{k=1}^{m} (\varepsilon_k \cdot \eta_k \cdot \Gamma_k) \tag{6}$$

in which

m	number of vulnerability indicators
$\Gamma_k \in [0,1]$	k-th vulnerability indicator
$\psi_k \in [0,1]$	relevance coefficient for the k-th vulnerability indicator

$$\eta_k = \frac{\psi_k}{\sum_{k=1}^{m} \psi_k} \tag{7}$$

and ε_k is a binary variable, which is equal to 0 if $\psi_k \quad \Gamma_k = 0$, and is equal to 1 otherwise.

Vulnerability factors Γ_k are calculated by converting those damage indicators expressed on a 1–5 scale (i.e., D-MS, D-FL, D-PW, D-IW, and D-IS) to the [0,1] range by

$$\Gamma_k = 0.25(G_k - 1) \tag{8}$$

For the damage indicators D-ES and D-RW, $\Gamma_k = G_k$. Relevance factors ψ_k were assigned based on personal communications with
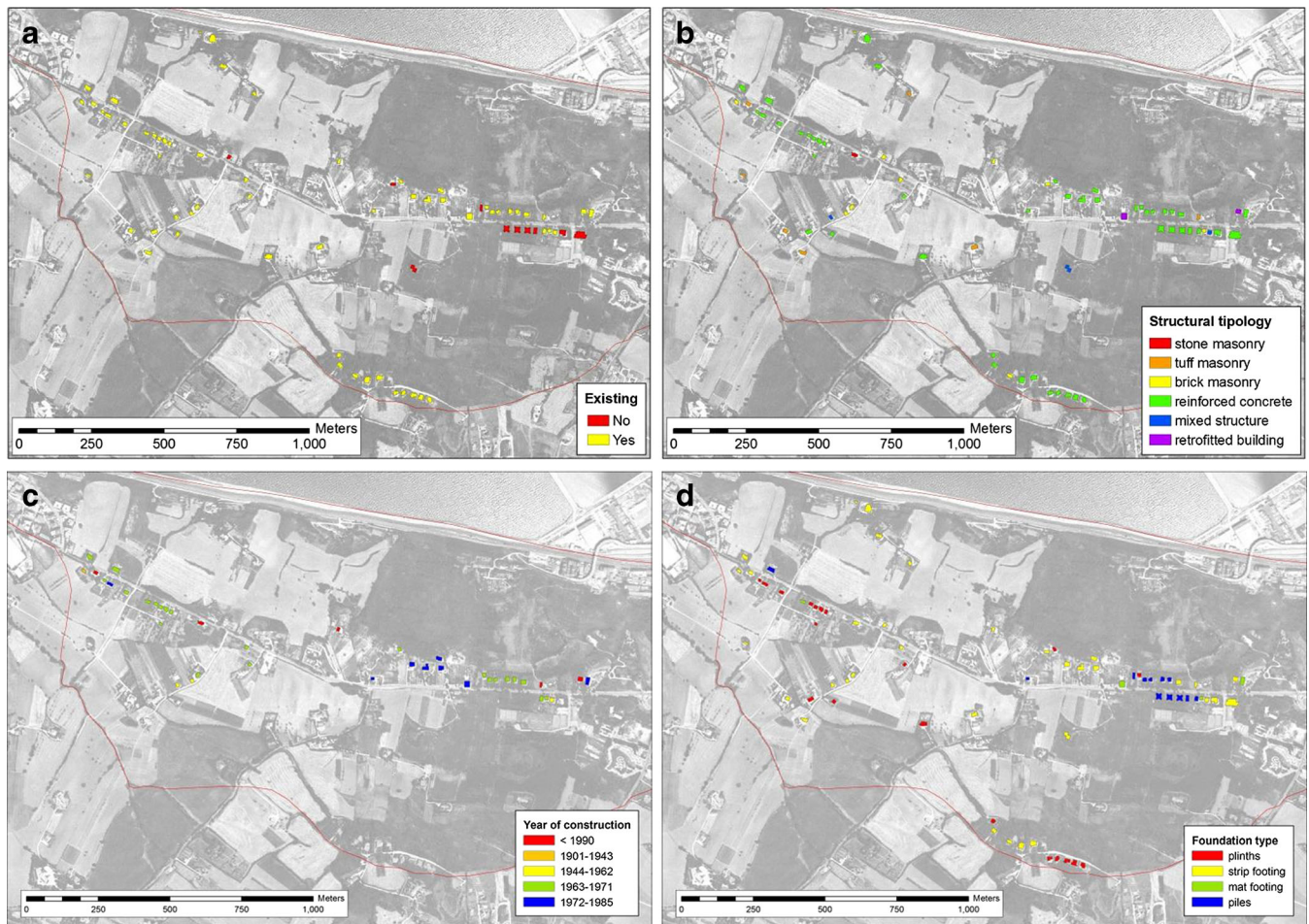

Fig. 2 Categorization of the 70 buildings surveyed in 1985–1986 by: **a** present-day existence, **b** structural typology, **c** age, and **d** foundation type
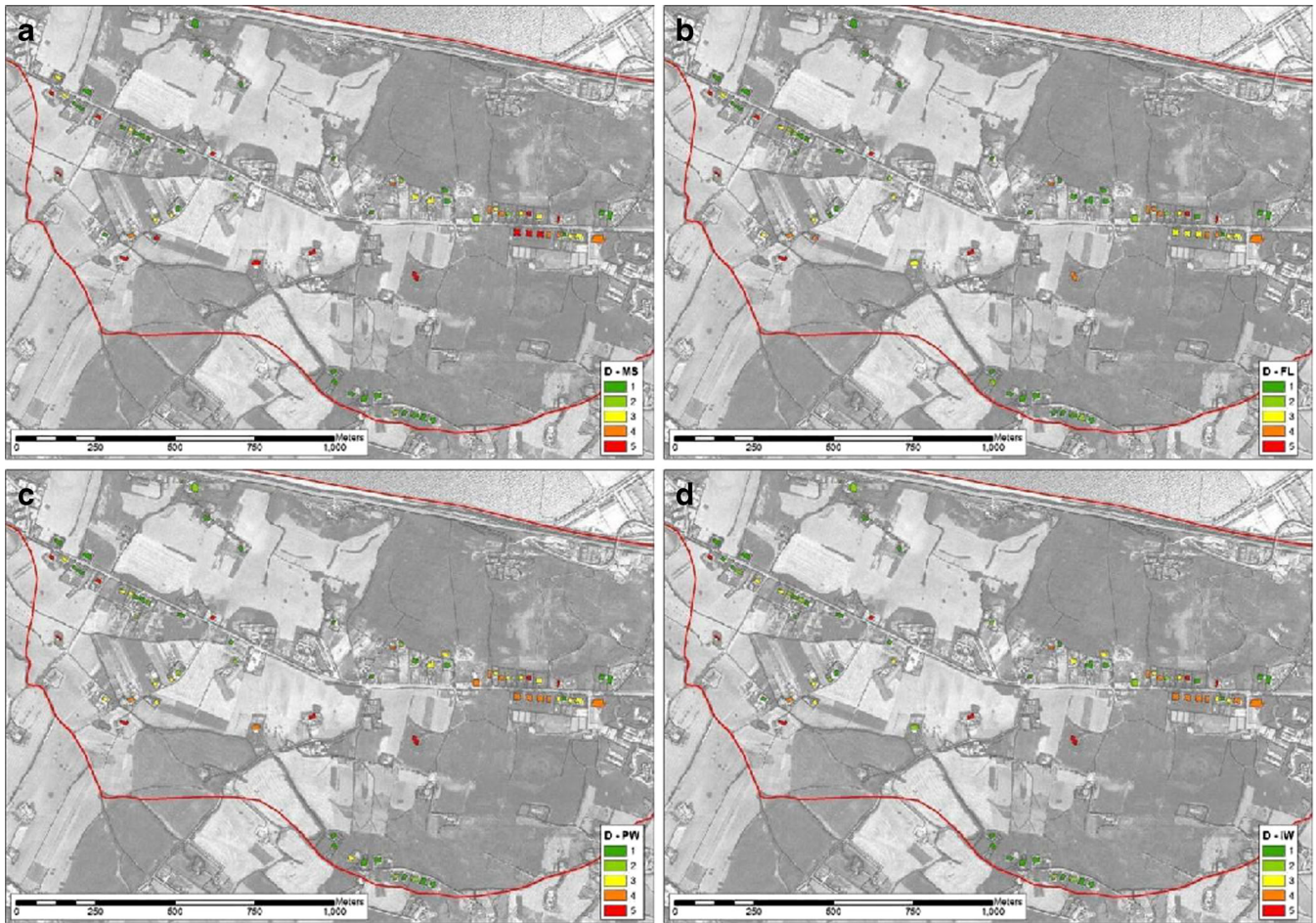
Fig. 3 Observed damage to the 70 buildings surveyed in 1985–1986: **a** main structures, **b** floors, **c** perimeter walls, and **d** internal walls

the technicians of the Ancona municipality, from reviews of the technical literature and, where necessary, using expert judgment. The values adopted in this study are shown in Table 1. Figure 5 plots the posterior vulnerability values calculated from Eq. (6) for the set of 70 surveyed buildings.

Estimation of building resilience

As stated previously, resilience parameterizes the inherent capability of vulnerable elements to preserve integrity, functionality, and desired performance in the course of the interaction with a reference hazardous event. Uzielli et al. (2008) introduced a general susceptibility model as well as models for susceptibility factors pertaining to specific categories of vulnerable elements. These models stemmed from data from past studies and/or from the quantitative parameterization of qualitative reasoning from reported findings and experience. Li et al. (2010) correspondingly introduced resistance models. As the original data from the source studies was very seldom collected, structured, and presented in a form directly usable for quantitative vulnerability estimation, models and magnitudes of resilience factors are invariably subjective and require progressive refinement through calibration and application to case studies. In addition, the models proposed in the above contributions did not allow the user to specify the relevance of each factor in determining the overall susceptibility or resistance. In

quantitative terms, factors that were less relevant were given implicitly the same weight as factors that could be expected to affect overall susceptibility (or resistance) to a larger degree. Here, the following resilience index model for buildings is introduced:

$$\Omega = \sum_{j=1}^{n} \left(\delta_j \cdot \rho_j \cdot \Theta_j \right) \tag{9}$$

where

n	number of resilience indicators
$\Theta_j \in [0,1]$	j-th resilience indicator
$\varphi_j \in [0,1]$	relevance coefficient for the j-th resilience indicator

$$\rho_j = \frac{\varphi_j}{\sum_{j=1}^{n} \varphi_j} \tag{10}$$

and δ_j is a binary variable

$$\delta_j = \mathrm{sign}\left(\varphi_j \cdot \Theta_j \right) \tag{11}$$

i.e., which is equal to 0 if $\varphi_j \quad \Theta_k = 0$, and is equal to 1 otherwise.
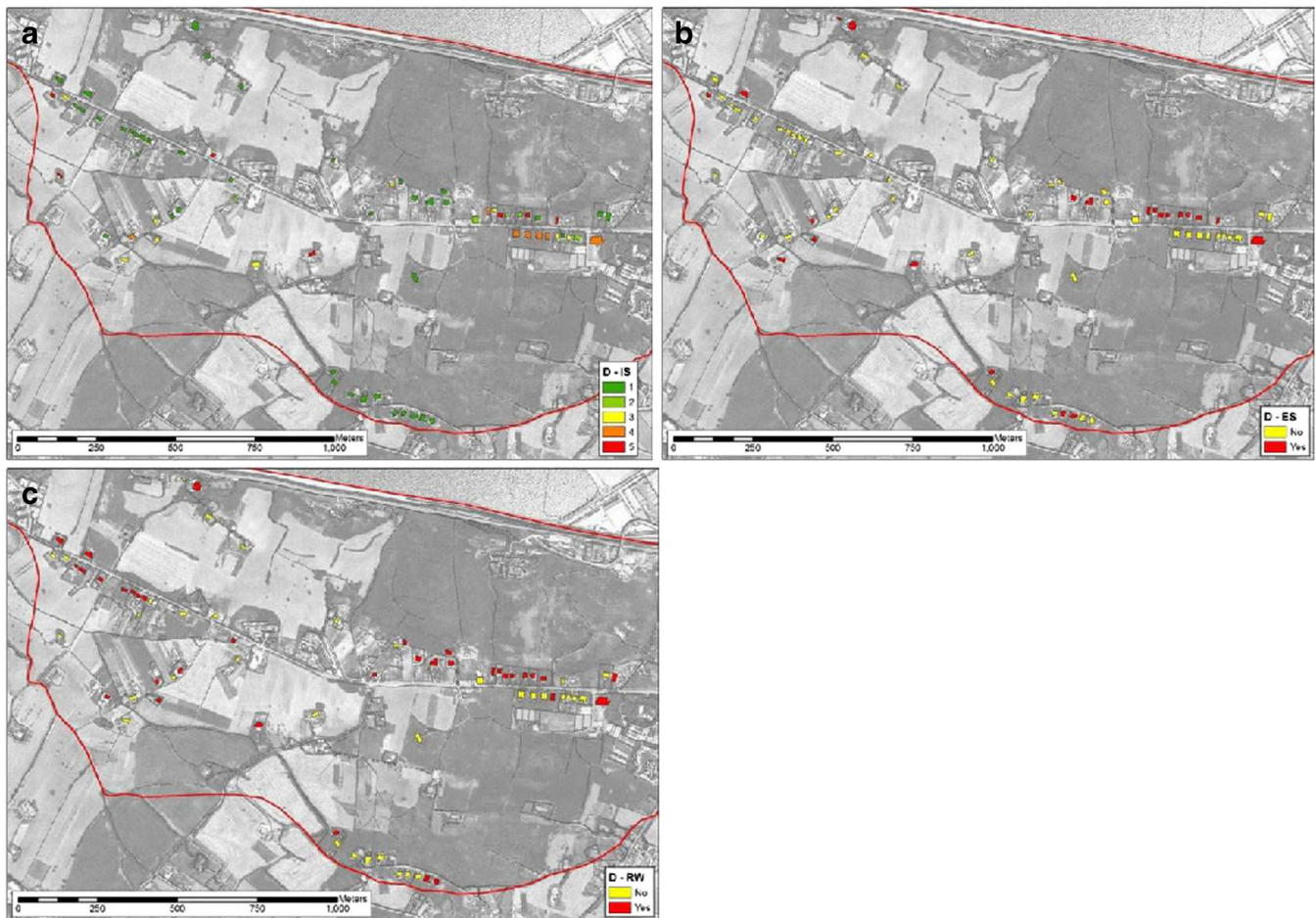
Fig. 4 Observed damage to the 70 buildings surveyed in 1985–1986: **a** internal staircases, **b** external staircases, and **c** retaining walls

Relevance coefficients are user-defined in the range [0,1] and reflect available knowledge or belief regarding the relevance of each indicator in concurring to damage. As the total resilience must be defined in the range (0,1], at least one of the resilience coefficients must be greater than 0. Detailed specification of relevance coefficients for intensity and resilience is optional: if, due to insufficient prior information, it is not possible to define a hierarchy in intensity and resilience indicators, relevance coefficients can be set uniformly equal to unity. Relevance coefficients are event specific (i.e., depending on the type of landslide) and

category specific (i.e., depending on the object of risk analysis). For instance, it could be known (or assumed) that the damage caused by a slow-moving landslide on a building is mainly due to the displacement (i.e., a geometric parameter), while kinetic characteristics could be predominant in case of a rapid movement.

A set of three resilience indicators (for the relevant attributes available in the damage survey) for landslide risk to structures are proposed; namely: (1) structural typology indicator Θ_{STY}, (2) building age indicator Θ_{AGE}, and (3) foundation type indicator Θ_{FNT}. These were selected as primary and most relevant indicators because (a) information pertaining to them was available from the post-damage survey and (2) they have been identified as ranking among the most relevant indicators by previous studies (e.g., Ragozin and Tikhvinsky 2000; Spence et al. 2005). Dai et al. (2002) opined that the quantitative assignment of vulnerability factors is significantly dependent on the type of landslide and vulnerable elements which vulnerability is calculated, and that it may consequently be a prevalently subjective process. The resilience indicator for foundation type accounts for both the ability of the foundation system to resist displacement and for its capability of preserving a rigid body behavior of the superstructure. Resilience indicators and relevance factors for the post-event state (i.e., at the time of the damage survey) were assigned as detailed in Tables 2, 3, and 4 based on a literature survey and on the critical analysis of the values previously adopted by Uzielli et al. (2008)

Table 1 Relevance factors for structural damage to Ancona buildings by components

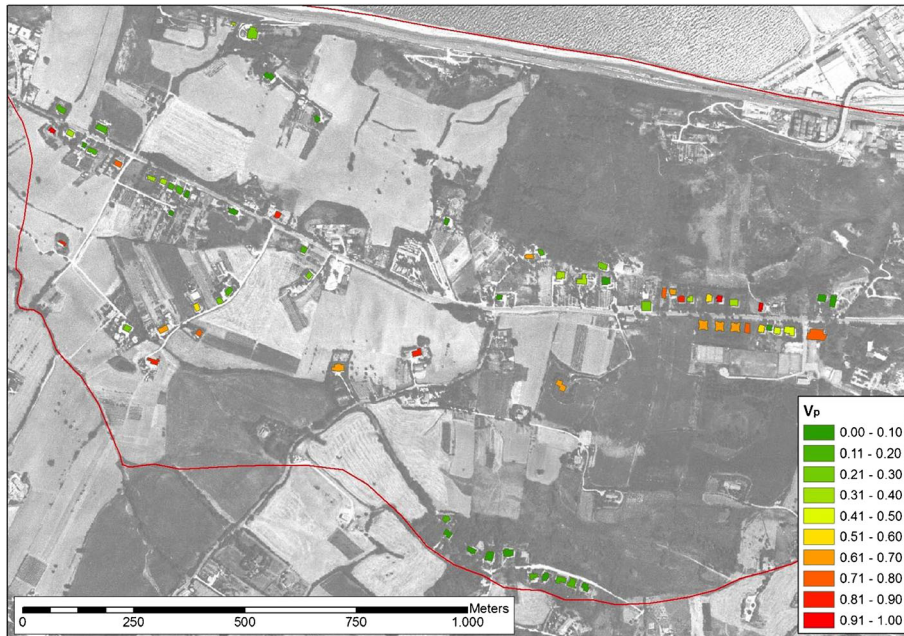|	Structural component	Ψ_k
MS	Main structure	1.00
FL	Floors	0.90
PW	Perimeter walls	0.80
IW	Internal walls	0.70
IS	Internal stairs	0.60
ES	External stairs	0.30
RW	Retaining walls	0.40

Fig. 5 Posterior vulnerability of the 70 buildings surveyed in 1985–1986

and Li et al. (2010). Figure 6 plots the post-event resilience Ω_p (i.e., the estimated resilience at the time of the post-event survey), calculated using the model in Eq. (9) using the indicators and relevance coefficients as described above, for the set of surveyed buildings.

Back-calculation of landslide intensity

The intensity model in Eq. (5) was implemented for the set of 70 buildings for which post-event survey data were available. Figure 7 plots the back-calculated posterior intensity for each of the 70 surveyed buildings.

Formulation of an intensity model

In order to perform a risk analysis for the target set of 39 buildings, it is necessary to formulate a quantitative model relating intensity to one or more geometric and/or kinetic parameters. In the case of the slow-moving Ancona landslide, kinetic attributes are deemed negligible in terms of damage potential. Back-calculated intensity was thus related to the displacements induced by the 13 December 1982 event. For the present study, an analytical intensity model was

developed empirically by comparing estimates of landslide-induced ground displacements for the 13 December 1982 event and the effects on the set of 70 buildings. Figure 8 (Anon 1986) plots the principal horizontal and vertical displacements which occurred in the hours immediately following the reactivation of the slide on 13 December 1982. Ground displacement estimates were obtained by comparing pre- and post-landslide aerial photographs as detailed in Cotecchia (2006). Displacement vectors were digitized and processed in a GIS environment to retrieve approximate quantitative values, which were subsequently examined jointly with the estimates of posterior vulnerability obtained in "Estimation of posterior vulnerability."

In order to relate post-event ground displacement to building damage, it is necessary to estimate the magnitude of observed vertical and horizontal ground displacements at building locations. As building locations generally do not correspond to displacement measurement locations, it is necessary to spatialize horizontal and vertical displacements through geostatistical interpolation of measured values. As in Uzielli et al. (2014), radial basis functions (RBF) with regularized splines are employed. The

Table 2 Resilience indicators and relevance factors for structural types for the Ancona buildings as categorized in the 1985–1986 damage survey

	Structural typology	Θ_{STY}	φ_{STY}
1	Stone masonry	0.30	1.00
2	Tuff masonry	0.40	1.00
3	Brick masonry	0.50	1.00
4	Reinforced concrete	0.70	1.00
5	Mixed structure	0.30	1.00
6	Retrofitted building	0.80	1.00

Table 3 Resilience indicators and relevance factors for age of buildings as categorized in the 1985–1986 damage survey

	Construction year	Age at time of survey	Θ_{AGE}	φ_{AGE}
1	<1900	>85	0.20	0.80
2	1901–1943	42–84	0.40	0.80
3	1944–1962	23–41	0.70	0.80
4	1963–1971	14–22	0.80	0.80
5	1972–1985	<13	0.90	0.80
6	Unknown	Unknown	0.20	0.80

Table 4 Resilience indicators and relevance factors for foundation type as categorized in the 1985–1986 damage survey

	Foundation type	Θ_{FNT}	φ_{FNT}
1	Plinths	0.10	0.90
2	Strip footing	0.30	0.90
3	Mat footing	0.50	0.90
4	Piles	0.70	0.90

magnitude of the total observed ground displacement vector is calculated as

$$D_{\mathrm{Gp,tot}} = \sqrt{D_{\mathrm{Gp,ver}}^2 + D_{\mathrm{Gp,hor}}^2} \qquad (12)$$

in which $D_{\mathrm{Gp,ver}}$ and $D_{\mathrm{Gp,hor}}$ are the vertical and horizontal components of displacement, respectively. The RBF interpolations of $D_{\mathrm{Gp,hor}}$, $D_{\mathrm{Gp,ver}}$, and $D_{\mathrm{Gp,tot}}$ are shown in Fig. 9a–c, respectively. It should be noted that only the magnitude of displacement vectors is of interest for the purpose of risk analysis, as damaging potential to buildings is assumed invariant to the direction of ground displacement.

A reference intensity model is obtained by subjectively fitting a power-law function to total observed post-event displacement and posterior intensity values for the 70 surveyed buildings. The analytical expression for intensity is thus

$$I = 0.22 \cdot D_{\mathrm{Gtot}}^{0.73} \qquad (13)$$

where D_{Gtot} is no longer the posterior displacement, rather a user-input value of total predicted ground displacement for forward

intensity estimation. The fitted curve provides an upper bound to data, with model coefficients resulting empirically from the upper-bound condition. The resulting model is conservative with respect to available sample data of back-calculated intensity and interpolated ground displacement. A conservative model is warranted by the presence of uncertainties in at least (a) the magnitude of ground displacement at building locations and (b) the kinematic interaction between ground and buildings. In the case of the Ancona landslide, it is assumed that the simplified, translational, rigid body movement of a building does not exceed that of the underlying soil volume. Figure 10 plots the posterior intensity I_p obtained in the section "Back-calculation of landslide intensity" versus the interpolated estimates of total ground displacement at the locations of the 70 surveyed buildings, as well as the analytical intensity model given in Eq. (13).

Estimation of specific risk

This section details the estimation of specific risk for a target set of 39 among the 70 surveyed buildings addressed in the previous sections. Target buildings were identified on the basis of two criteria: (1) they are existing and (2) they are sufficiently close to monitoring locations (inclinometers and interferometer targets) to allow relatively confident estimation of ground displacement from geostatistical interpolation as discussed in Uzielli et al. (2014).

Total ground displacement model

As discussed previously, the estimation of specific risk relies on the modeling of hazard and vulnerability as functions of total ground displacement. Operationally, specific risk for a building and for a time interval T is given by the summation of the product of hazard
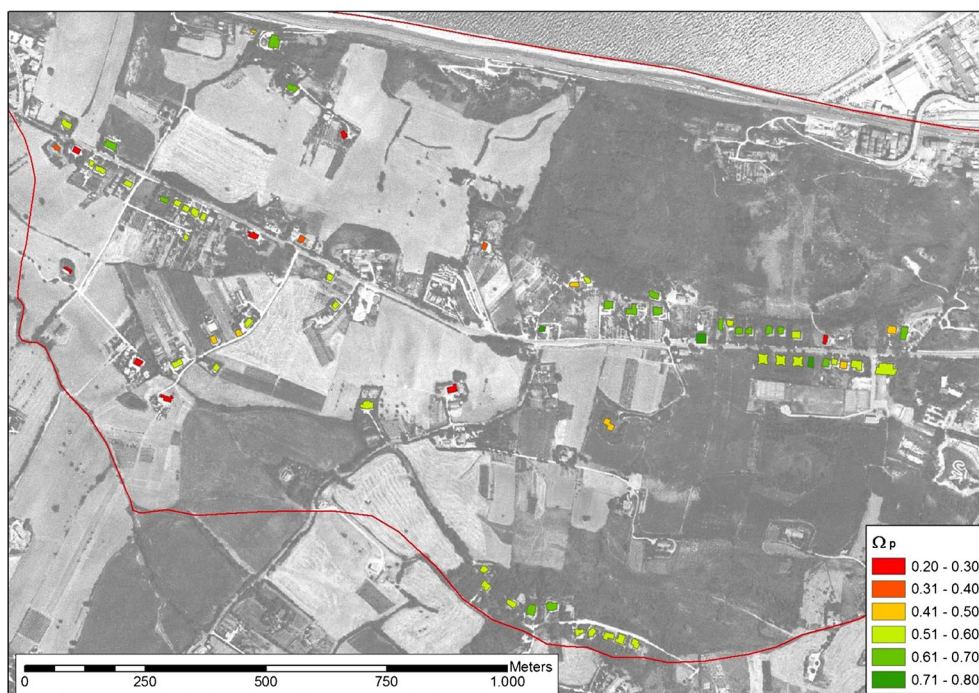

Fig. 6 Posterior resilience of the 70 buildings surveyed in 1985–1986
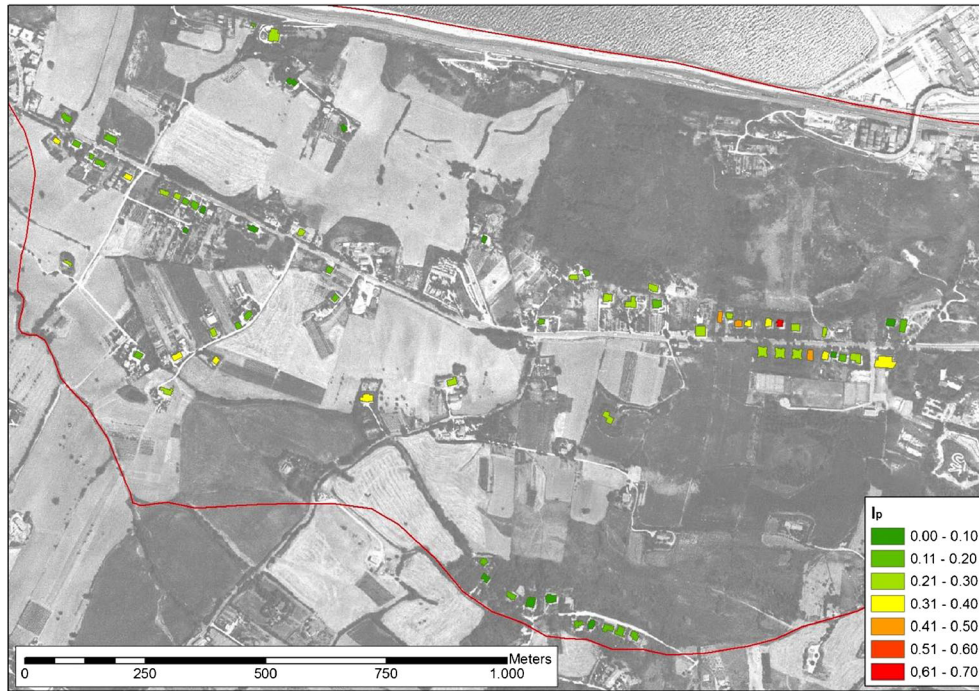
Fig. 7 Back-calculated landslide intensity of the landslide event of 13 December 1982 at the locations of the 70 buildings surveyed in 1985–1986

and vulnerability calculated at all plausible ground displacement levels at the location of the building:

$$R_{s,T} = \sum_{i=1}^{N_{D,T}} H_i\big(D_{Gtot,T}\big) \cdot V_i\big(D_{Gtot,T}\big) \qquad (14)$$

where, for a given time interval T, $N_{D,T}$ is the (discrete) number of operational total ground displacement levels at which hazard and vulnerability are estimated. Equation (14) highlights the

dependence of hazard and vulnerability on the reference time interval T. The magnitude of total ground displacement is then given by

$$D_{Gtot,T} = \sqrt{D_{Ghor,T}{}^2 + D_{Gver,T}{}^2} \qquad (15)$$

in which $D_{Ghor,T}$ and $D_{Gver,T}$ are the horizontal and vertical ground displacements, respectively. These are estimated independently as
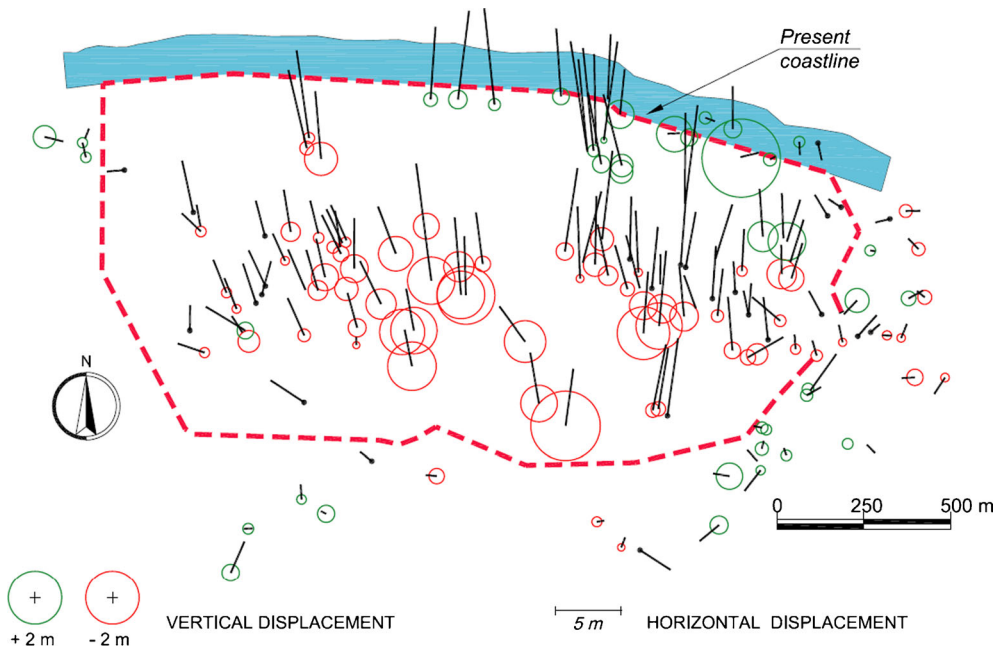
Fig. 8 Measured horizontal and vertical displacements resulting from the 13 December 1982 event (Anon 1986)
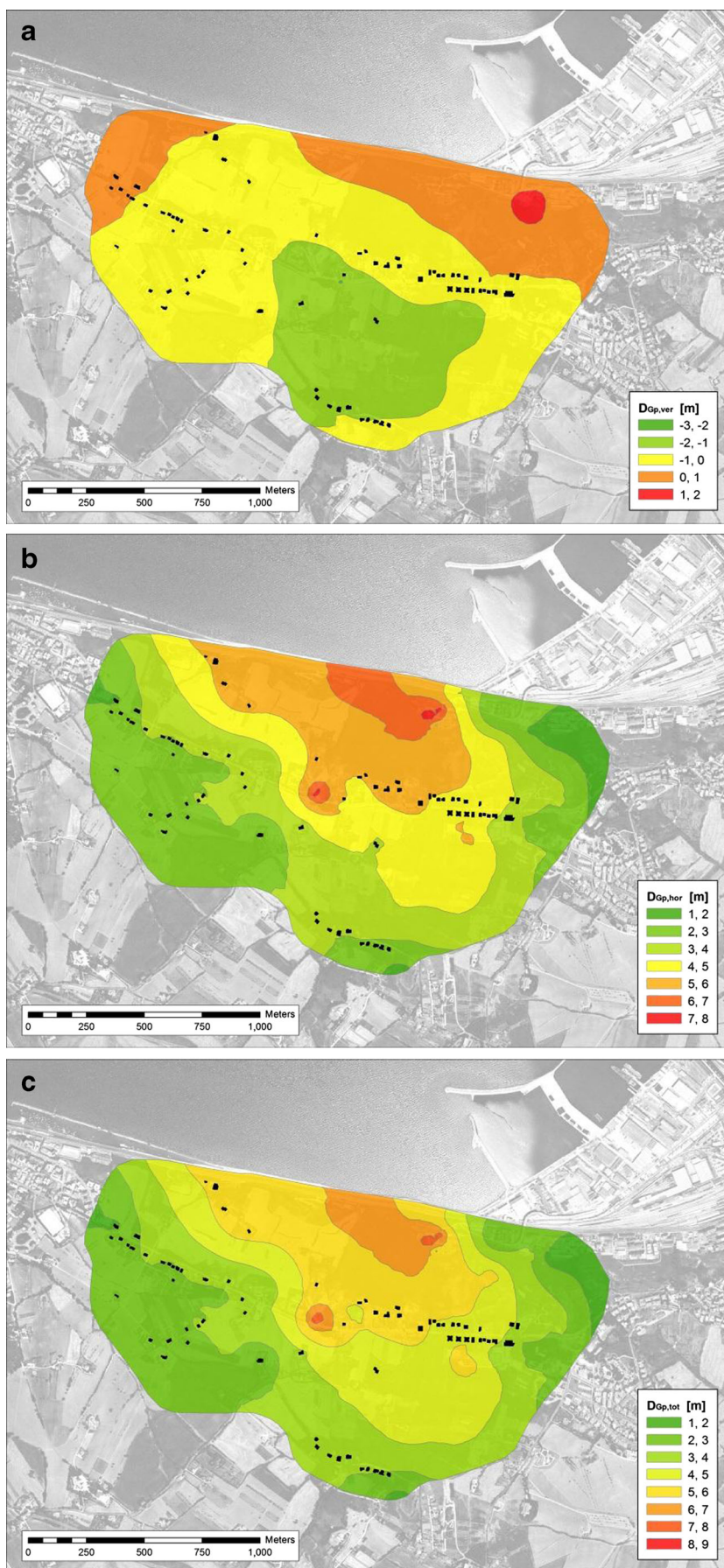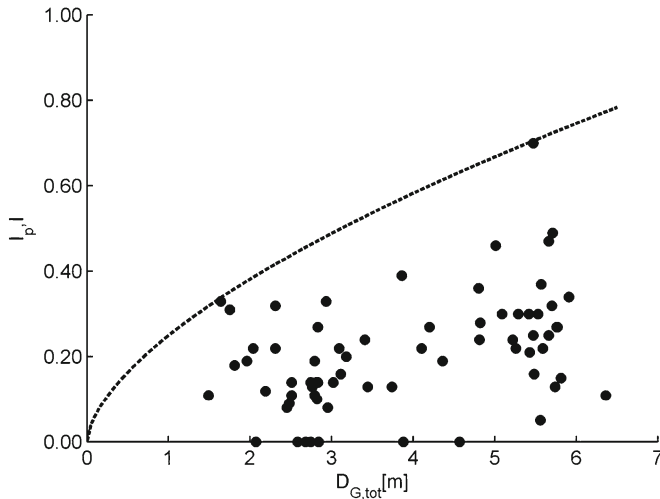
Fig. 10 Posterior intensity values from the 13 December 1982 event on the 70 surveyed buildings and reference intensity model versus total ground displacement

described in "Simulation of horizontal ground displacement" based on the outputs of the statistical analysis of horizontal yearly velocity (from inclinometer data) and vertical yearly velocity (from radar interferometer PSInSAR^{TM} data) as detailed in Uzielli et al. (2014). In this study, five reference time intervals are investigated: 1, 10, 25, 50, and 100 years. For the sake of conciseness, these reference intervals are occasionally referred to as T001, T010, T025, T050, and T100, respectively, in figures and tables.

Hazard estimation

With reference to the definition given in the "Reference risk model" section, hazard corresponds to the probability of occurrence, in the reference time interval, of a hazardous event of a given magnitude. Here, ground displacement D_G serves as the reference hazardous attribute of the landslide. Displacement was estimated through the statistical calculation and subsequent

probabilistic Monte Carlo simulation of the average horizontal and vertical yearly velocities.

Simulation of horizontal ground displacement

With reference to the statistical analysis of inclinometer data presented in Uzielli et al. (2014), the aggregate horizontal displacement $D_{Ghor,T}$ measured at one inclinometer location in a reference time interval T is calculated by

$$D_{Ghor,T} = \sum_{j=1}^{T} \left| \xi_{Ghor,j} \right| \tag{16}$$

in which $\xi_{Ghor,j}$ is the average yearly horizontal ground velocity in the j-th year ($j=1,\dots, T$) at a depth of 1 m below ground level as detailed in Uzielli et al. (2014). Note that the notation ξ_{Ghor} replaces the notation ξ_{IN} used in the companion paper. Probabilistic simulation was employed to estimate $D_{Ghor,T}$ from Eq. (16), which thus represents an additive model. The equation should be regarded as a vector equation in which T vectors $|\xi_{Ghor,j}|$, each of size n_{sim}, are added. Vectors correspond, for each inclinometer and reference time interval, to sampling distributions of ξ_{Ghor}. Sampling distributions were generated nonparametrically, i.e., not according to preset distribution types; rather, they were based on the empirical cumulative distribution functions (ECDFs) of ξ_{Ghor} obtained in Uzielli et al. (2014). A size $n_{sim}=10,000$ was established for all sampling distributions. The output of Eq. (16) is a n_{sim}-sized vector, which corresponds, for a given period T, to a sample of aggregate horizontal ground displacement. The presence of absolute values in Eq. (16) reflects the conservative hypothesis by which displacement-induced damage is invariant to the direction of ground movement. The inherent conservatism lies in the fact that, by summation of absolute values, $D_{Ghor,T}$ is maximized for any given set of sampled values.

The estimation of specific risk for long reference time intervals implies the hypothesis of temporal stationarity of slope kinematic parameters, i.e., the belief that slope movements will not change significantly in time. This hypothesis was verified by checking the absence of significant temporal trends (i.e., accelerations or decelerations) in ξ_{Ghor} for the monitoring period for which data were
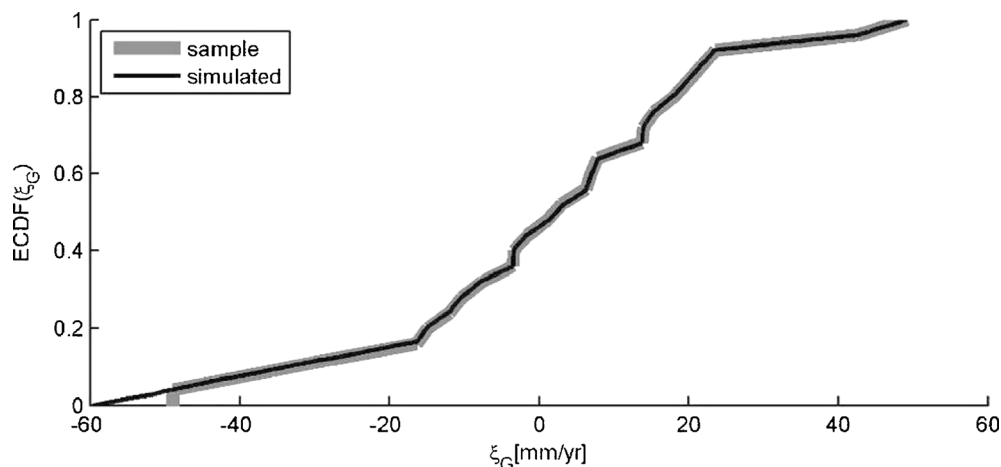

Fig. 11 Empirical cumulative distribution function of measurement sample and simulated sets of horizontal ground velocity for one of the inclinometers located inside the landslide area
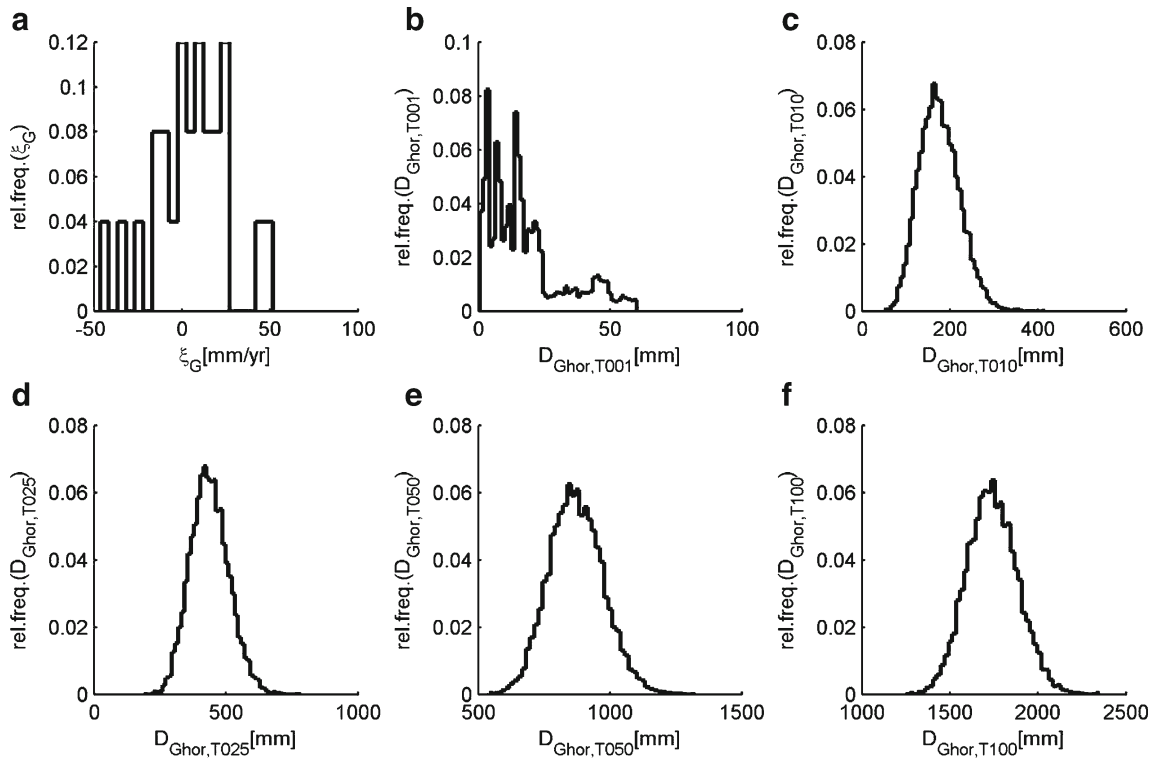
Fig. 12 Example relative frequency histograms of **a** input sampling distribution of ξG and output samples of horizontal ground velocity *D*Ghor for time periods of **b** 1 year, **c** 10 years, **d** 25 years, **e** 50 years, and **f** 100 years for an inclinometer

available (2002–2008) through the calculation of Kendall's tau statistic. It was assessed that no significant trends were present in any of the velocity time series. As will be discussed in the "Summary and concluding remarks" section, no exceptional
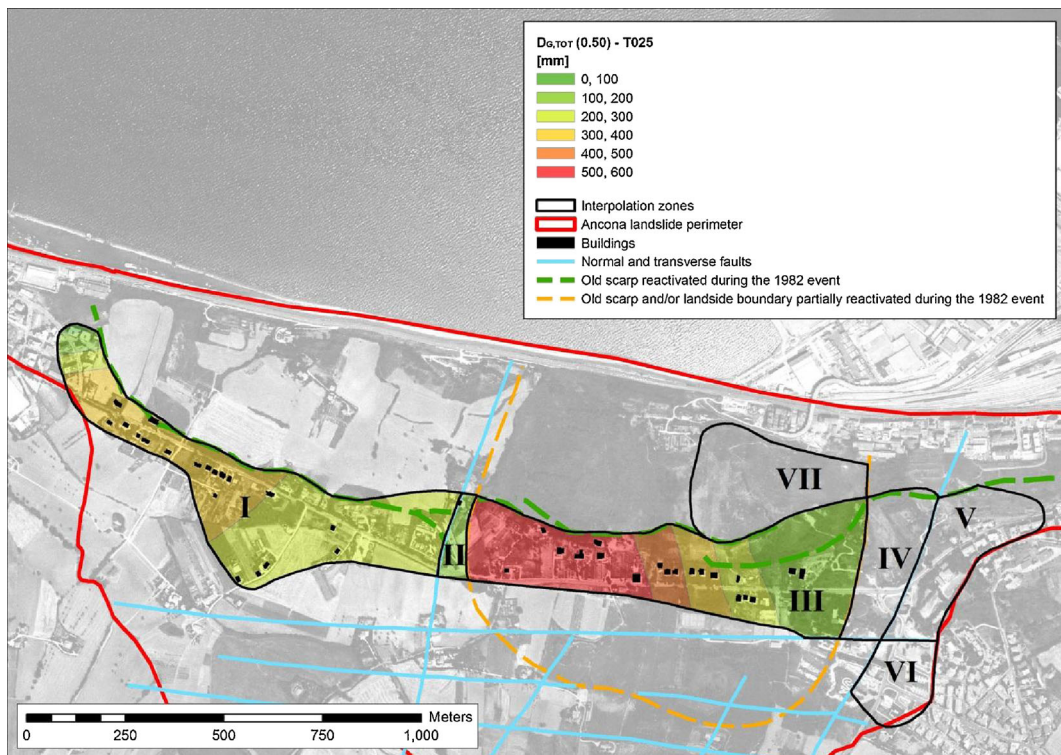
Fig. 13 Radial basis interpolation of median total ground displacement for a reference time interval of 25 years
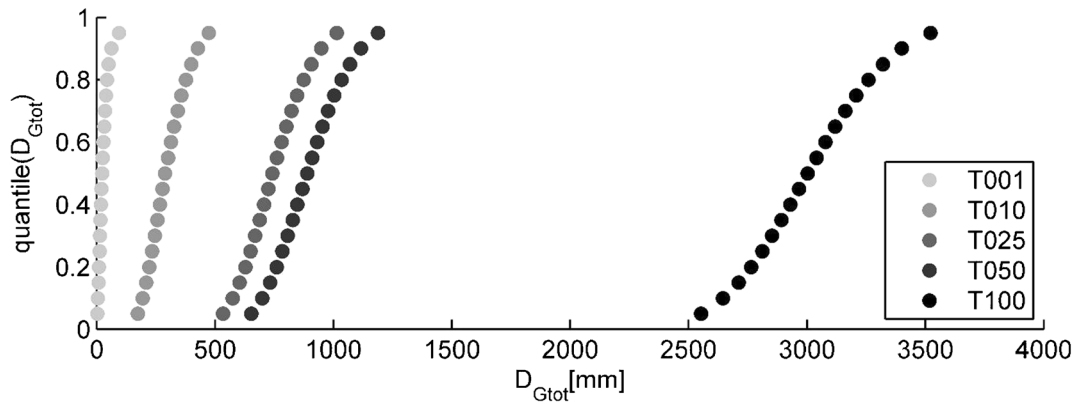
Fig. 14 Sets of quantiles of total ground displacement DGtot at one of the target buildings for time periods of 1, 10, 25, 50, and 100 years

sliding scenarios such as the 13 December 1982 event occurred during the monitoring period. The projection of the hypothesis of temporal stationarity beyond the monitoring period for future risk analysis entails that the resulting risk estimates should not be considered upper-bound estimates. The main conceptual utility of the present analysis thus lies in the assessment whether non-exceptional hazard scenarios are tolerable/acceptable in terms of risk to buildings. Figure 11 plots an example, for one of the inclinometers located within the landslide perimeter, of (a) the empirical cumulative distribution function of ξ_{Ghor} and (b) the cumulative distribution function of the generated size—10,000 sampling distribution of ξ_{Ghor}. Figure 12 plots (a) the relative frequency histogram of the input sampling distribution of ξ_{Ghor} and the relative frequency histograms of the output samples of D_G for: (b) 1 year, (c) 10 years, (d) 25 years, (e) 50 years, and (f) 100 years for the same inclinometer. It should be noted that all values of the output distribution are positive because absolute values are considered in Eq. (16). Also, the distribution of output samples approaches a Gaussian shape with increasing period T in accordance with the central limit theorem, by which the sum of a large number of random variates (in the present case, the nonparametric sampling distributions) with finite variance approaches a Gaussian distribution.

Sets of 19 sample quantiles of $D_{Ghor,T}$ were retrieved for each inclinometer and for each reference time interval T from the simulation output samples of D_{Ghor} calculated by probabilistic

simulation: namely, the 0.05, 0.10, 0.15, 0.20, 0.25, 0.30, 0.35, 0.40, 0.45, 0.50, 0.55, 0.60, 0.65, 0.70, 0.75, 0.80, 0.85, 0.90, and 0.95 quantiles. The above procedure allows the statistical and probabilistic processing of ground displacement data at inclinometers locations. For risk estimation purposes, it is necessary to estimate the same parameters at building locations. This indirect estimation is pursued by radial basis (RBF) interpolation. All displacement quantiles were interpolated inside the landslide perimeter for the five reference time intervals.

The vertical component of ground displacement was estimated analogously by processing measurements of vertical velocity taken at pseudolocations of permanent scatterers for ENVISAT satellite readings as detailed in Uzielli et al. (2014). The aggregate vertical displacement $D_{Ghor,T}$ measured at one pseudolocation in a reference time interval T is given by

$$D_{Gver,T} = \sum_{j=1}^{T} \left| \xi_{Gver,j} \right| \qquad (17)$$

in which $\xi_{Gver,j}$ is the vertical yearly ground velocity in the j-th year ($j=1,\ldots, T$) estimated from PSInSAR interferometer data as detailed in Uzielli et al. (2014). The simulation procedure was performed as described for horizontal velocity, and vertical ground displacement was spatialized at the 39 building locations.

Figure 13 plots the interpolation of the median quantile of D_{Gtot} for a 25-year interval. The figure also shows the seven interpolation
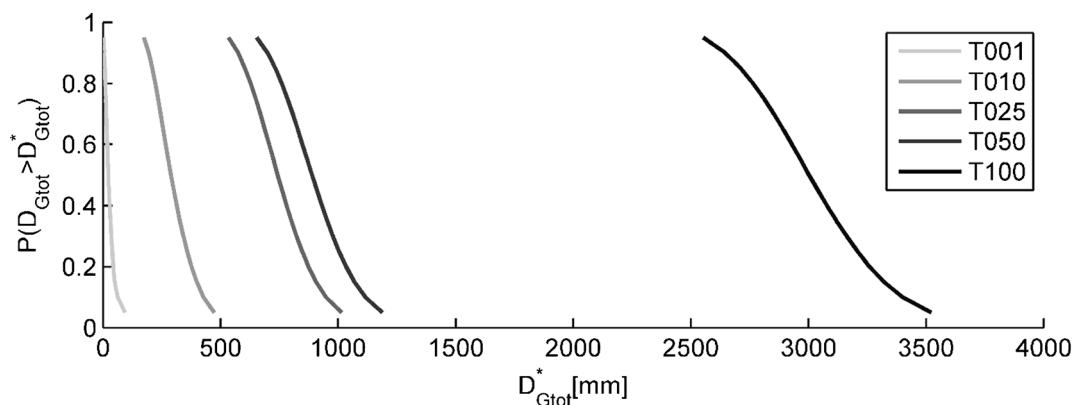

Fig. 15 Displacement exceedance probability curves for one of the target buildings by reference time interval (1, 10, 25, 50, and 100 years)

Table 5 Variation in the resilience factor for building age Θ_{AGE} by category of buildings and reference time interval

Cat.	Time of survey		1 year		10 years		25 years		50 years		100 years	
	Age	Θ_{AGE}	Age	Θ_{AGE}	Age	Θ_{AGE}	Age	Θ_{AGE}	Age	Θ_{AGE}	Age	Θ_{AGE}
1	100	0.20	125	0.20	135	0.17	150	0.14	175	0.10	225	0.05
2	80	0.40	105	0.26	115	0.22	130	0.18	155	0.13	205	0.07
3	40	0.70	65	0.43	75	0.38	90	0.31	115	0.22	165	0.12
4	25	0.80	50	0.52	60	0.46	75	0.38	100	0.27	150	0.14
5	15	0.90	40	0.59	50	0.52	65	0.43	90	0.31	140	0.16
6	Unknown	0.20	125	0.20	135	0.17	150	0.14	175	0.10	225	0.05

subzones defined in Uzielli et al. (2014). These subzones reflect the tectonic and geomorphologic setting of the landslide, accounting for the possible spatial discontinuities in the displacement field due to the presence of normal and transverse faults and scarps which were totally or partially reactivated during the 1982 event. Interpolation of total displacement was performed only in those subzones containing target buildings, i.e., subzones I, II, and III. Interpolated values at building locations were retrieved. Figure 14 plots an example of the displacement quantiles extracted at the location of one of the target buildings for the five reference time intervals. For each building, quantiles were interpolated linearly between each couple of consecutive point values in order to obtain estimates with a displacement step of 1 mm. The resulting number N_D of displacement-quantile couples is building specific as it depends on the source range of displacements.

Calculation of hazard

Hazard descends directly from the outputs of probabilistic simulation of total displacement. Displacement exceedance probability curves were drawn for each building and for each reference time interval. Figure 15 shows an example plot of the exceedance probability for one of the target buildings by reference time interval. It should be noted that displacements are considered in discrete sets

(i.e., at integer millimeter values); hence, the exceedance probability curves are plotted as continuous lines solely for illustrative purposes. Hazard values were obtained by deconvolution of the cumulative exceedance probability curves, i.e., by subtracting values of the probability of exceedance for consecutive discrete displacement values, thereby obtaining the probability that displacement equals a preset magnitude.

Estimation of vulnerability

The vulnerability model in Eq. (4) is implemented in a forward analysis for the target set of 39 buildings. Intensity was calculated using Eq. (13) for each building and reference time interval. Input values of ground displacements were given by probabilistic simulation as described in "Hazard estimation.". The resilience index was estimated as detailed in "Estimation of building resilience."

It is important to note that the resilience of the buildings generally does not correspond with the values used in the back-calculation of intensity detailed in "Back-calculation of landslide intensity.". There, building resilience was estimated with reference to building conditions at the time of the damage survey (1985–1986). Since then, it can be expected that the resilience factor for building age has decreased due to progressive structural degradation in time. The following model is proposed for the resilience factor for building age:

$$\Theta_{AGE} = \exp(-0.013 \cdot age) \tag{18}$$

where age is expressed in years from the beginning of construction. The model was obtained through the comparative fitting of various analytical models to the values proposed by Li et al. (2010), which result from a critical review of available literature. The exponential formulation given in Eq. (18) displayed the best fit to the aforementioned data. Table 5 illustrates the variation in the resilience factor for building age Θ_{AGE} for each category of buildings and for each time interval.

As information regarding possible retrofitting of buildings is not available, it is conservatively assumed that neither retrofitting nor structural/geotechnical consolidation interventions have been performed since the 1985–1986 survey, nor will they be in the longest period for which specific risk is estimated (100 years). Consequently, the same values of the resilience factors for structural typology and foundation type used in "Estimation of building resilience" are adopted in the estimation of specific risk. Figure 16 plots the variation in resilience versus reference time interval for the target set of 39 buildings.
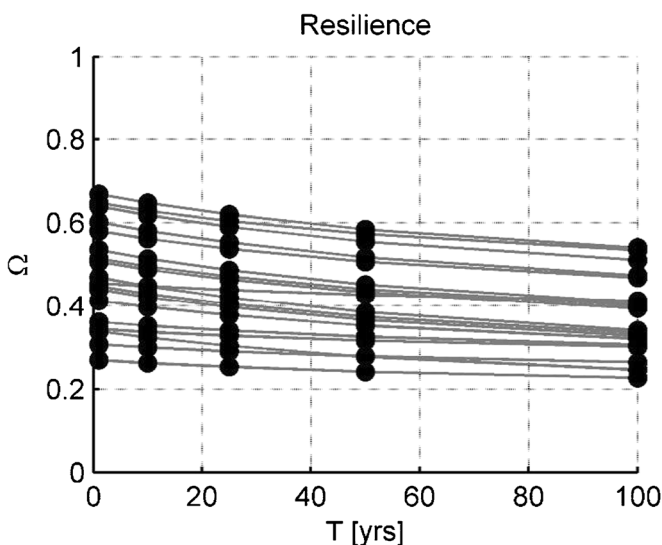

Fig. 16 Variation of resilience versus reference period for the set of 39 target buildings
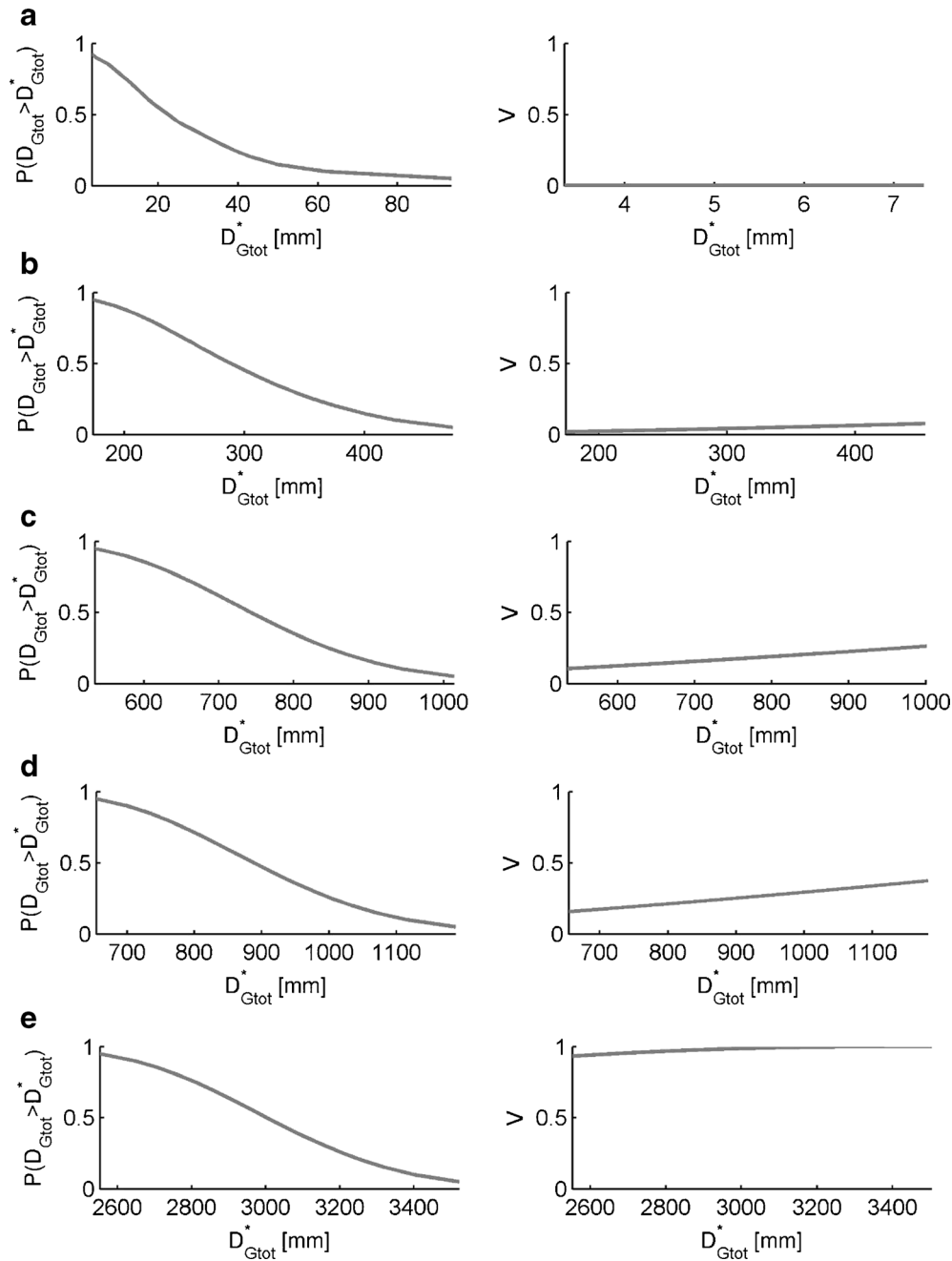
Fig. 17 Exceedance probability curves and vulnerability curves for one of the target buildings for time intervals of **a** 1 year, **b** 10 years, **c** 25 years, **d** 50 years, and **e** 100 years

Estimation of specific risk

The specific risk model given in Eq. (14) was implemented using the hazard and vulnerability values calculated as described in "Hazard estimation" and "Estimation of vulnerability," respectively. Figure 17 plots the exceedance probability curves and vulnerability curves for one of the 39 buildings for each of the five reference time intervals. The convolution, involving the sum of the scalar multiplications of the two vectors at each "possible" displacement value for a given reference time interval, yields the single estimate of R_S for the period itself. Specific risk is a useful parameter as it allows the immediate, intuitive prediction of the

percentage loss in value of a building in a reference time interval. For instance, a specific risk estimate of 0.15 for a 25-year interval is equivalent to the prediction by which 15 % of the building's value will be lost in the next 25 years. Estimates of specific risk for the five reference time intervals from 1 to 100 years are plotted in Figs. 18, 19, 20, 21, and 22. Figure 23 plots the variation of specific risk versus reference time interval for the set of buildings. As expected, specific risk increases significantly with the reference time interval, due to the increases both in hazard (due to the larger ground displacements which are more likely to occur during longer periods) and in vulnerability (due to the increase in
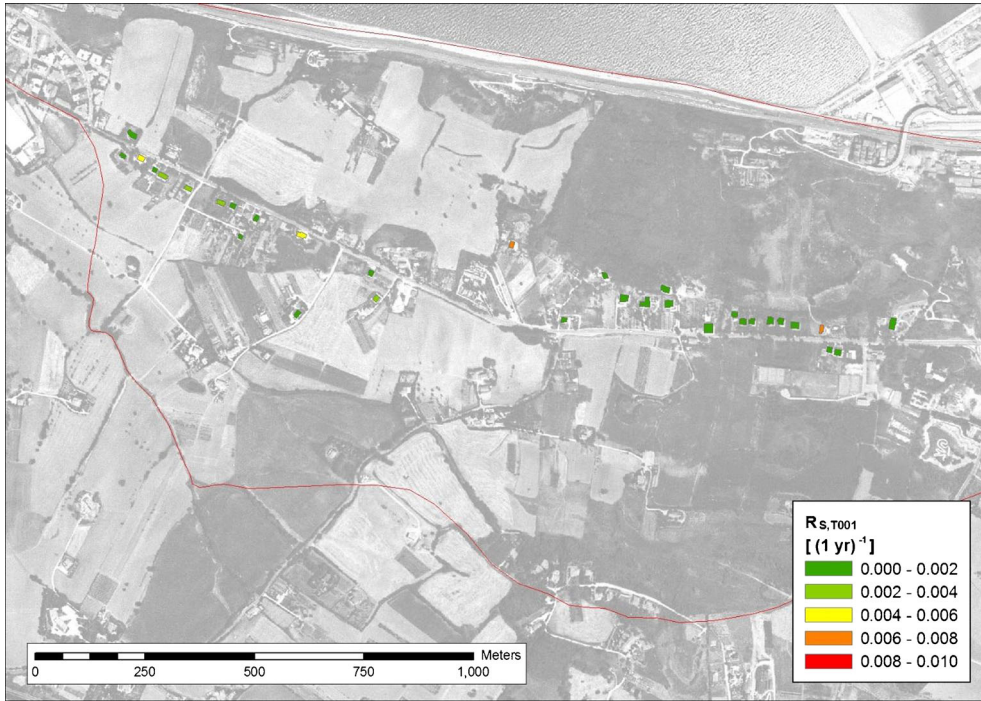
Fig. 18 Specific risk estimates for the 39 target buildings for a time interval of 1 year

displacement-related intensity and the decrease in resilience as a consequence of the aging of buildings). Considering the target set of 39 buildings, specific risk could be described overall as "negligible" for a 1-year interval; "low" for 10 years; "medium" for 25 years; "high" for 50 years and "extremely high", with values almost uniformly at the upper-bound value of unity, for 100 years. The scatter in specific risk estimates is low for 1-, 10-, and 100-year intervals; moderate for 25 years; and very large for 50 years. Some buildings display greater increase in R_S between 25- and 50-year intervals; others between 50 and 100 years.
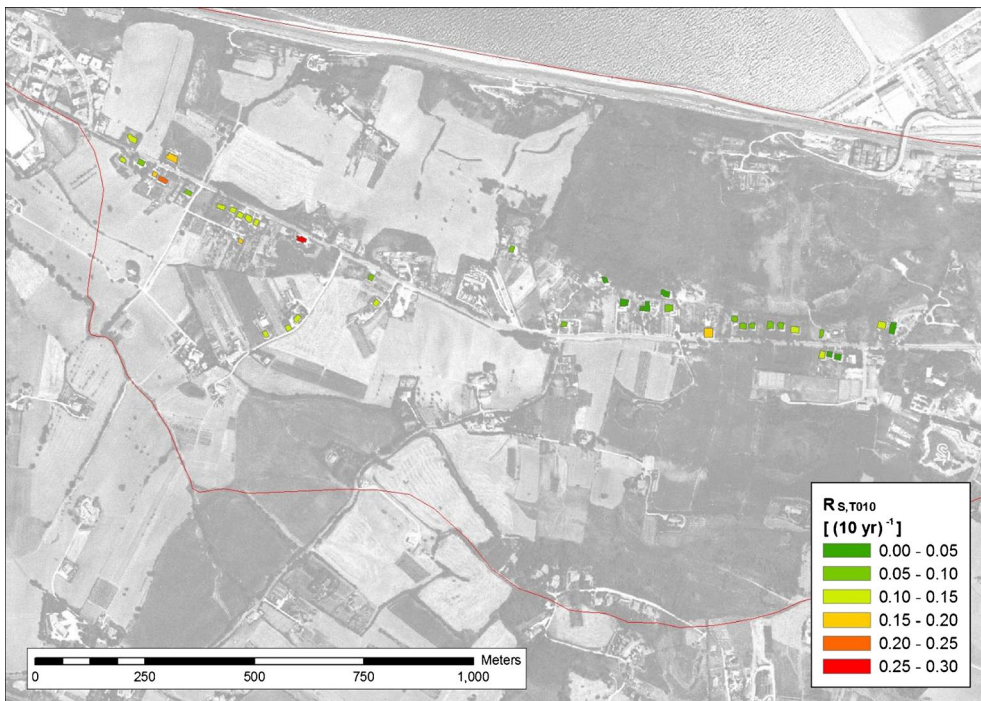
Fig. 19 Specific risk estimates for the 39 target buildings for a time interval of 10 years
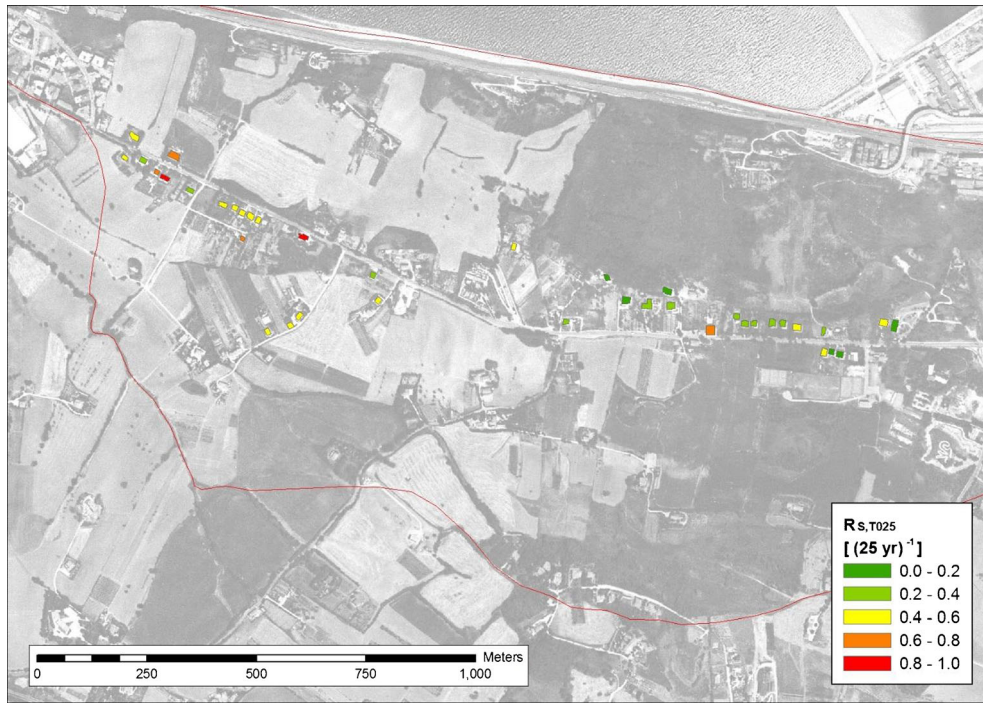
Fig. 20 Specific risk estimates for the 39 target buildings for a time interval of 25 years

From specific risk to risk

Referring to the model in Eq. (2), risk can be estimated from specific risk if estimates of the value of vulnerable elements are available. Such estimates were not available for the set of target buildings; hence, full risk estimation could not be attempted. As an illustrative example, however, suppose the estimated value of a building in a reference time interval of 25 years is E=€500,000 and the specific risk estimate for a 25-year interval is 0.13, the corresponding 25-year risk would be €65,000. It is worth noting that similar to hazard and vulnerability, E is period specific as it is

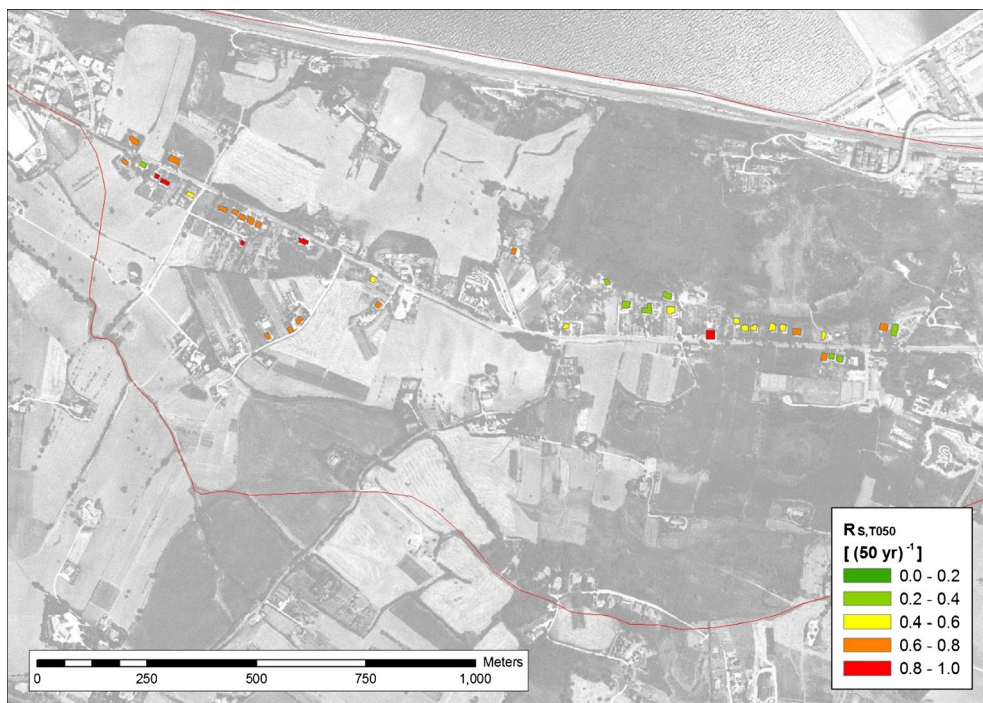**Fig. 21** Specific risk estimates for the 39 target buildings for a time interval of 50 years

Fig. 22 Specific risk estimates for the 39 target buildings for a time interval of 100 years

likely that the value of a building will change in time due, for instance, to market fluctuations and inherent value of the building following structural degradation or restoration.

Summary and concluding remarks

Specific risk as defined in the present study depends, both qualitatively and quantitatively, on the combined effect of the resilience of vulnerable elements and slope kinematics. Consequently, it is a complex parameter to be estimated. Due to the inherent complexity in the estimation of hazard and vulnerability, the quantitative estimates of specific risk obtained herein are pervaded by uncertainty.

The reduction of the epistemic components of uncertainty in hazard and vulnerability through additional monitoring data and/or improved vulnerability models is practically unattainable. Moreover, in the case of the Ancona landslide, the limited amount

Fig. 23 Variation of specific risk versus reference time interval for the set of 39 target buildings

of measurement points in the landslide area does not allow confident spatialization of hazard and vulnerability indicators by geostatistical interpolation. To avoid underestimation of specific risk, an upper-bound intensity model was employed in the calculation of vulnerability. This is a correct approach from an engineering standpoint in the presence of nonreducible uncertainty.

Overall, quantitative estimates are plausible in terms of consistency with qualitative observations and available information regarding slope kinematics and the characteristics of vulnerable elements, as given for instance in Cotecchia (2006). Buildings with low resilience and located in high-displacement locations display high specific risk, while high-resilience buildings located in low-displacement areas display low specific risk. Intuitively, the qualitative assessment of specific risk is less straightforward for the two intermediate cases, i.e., low-resilience buildings in low-displacement areas and high-resilience buildings in high-displacement areas. Therein lies the complexity and period dependence of risk estimates, which reflect the detailed statistical characterization of slope kinematics pursued in the study and the period-dependent variations in the factors of specific risk: intensity, resilience and, ultimately, hazard and vulnerability.

The risk estimates obtained herein can be considered as non-upper-bound values, since the monitoring data (inclinometer and interferometer) used to obtain the sampling distributions for the simulation of displacement over the five reference time intervals were collected between 2002 and 2008. During this period, no large-scale sliding events such as the one of 13 December 1982 occurred. Hence, there is the important result that even though the landslide is slow-moving, and even though the study does not include data from more extreme scenarios, estimated specific risk to buildings is not negligible even for intermediate time periods (10 years and up). The present case study thus highlights the importance of pursuing risk estimates from a quantitative
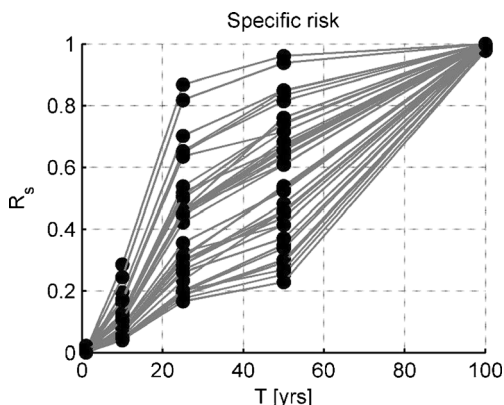
perspective, aiming to serve as a resource for rational risk management scheme of the Ancona urban area.

References

Agostini A, Tofani V, Nolesini T, Gigli G, Tanteri L, Rosi A, Cardellini S, Casagli N (2014) A new appraisal of the Ancona landslide based on geotechnical investigations and stability modelling. Quarterly Journal of Engineering Geology and Hydrogeology (http://dx.doi.org/10.1144/qjegh2013-028)

Amatruda G, Bonnard C, Castelli M, Forlati F, Giacomelli M, Morelli M, Paro L, Piana F, Pirulli M, Polino R, Prat P, Ramasco M, Scavia C, Bellardone G, Campus S, Durville JL, Poisel R, Preh A, Roth W, Tentschert EH (2004) A key approach: the IMIRILAND project method. In: Bonnard C, Forlati F, Scavia C (eds) Identification and mitigation of large landslide risks in Europe—advances in risk assessment. European Commission Fifth Framework Program. Balkema, Rotterdam, pp 13–44

Anon (1986) La grande frana di Ancona del 13 Dicembre 1982. Special issue of "Studi geologici Camerti", pp 146

Birkmann J (ed) (2006) Measuring vulnerability to natural hazards. United Nations University Press, New York, p 524

Catani F, Casagli N, Ermini L, Righini G, Menduni G (2005) Landslide hazard and risk mapping at catchment scale in the Arno River basin. Landslides 2(4):329–342

Cotecchia V (2006) Experience drawn from the great Ancona landslide of 1982. The second Hans Cloos Lecture. Bull Eng Geol Environ 65:1–41. doi:10.1007/s10064-005-0024-z

Dai FC, Lee CF, Ngai YY (2002) Landslide risk assessment and management: an overview. Eng Geol 64:65–87

Comune di Ancona (1985) Piano di recupero dell'area in frana—Schede analitiche (Damage survey)

Glade T, Anderson M, Crozier MJ (eds) (2005) Landslide hazard and risk. Wiley, New York, p 824

Ho KKS, Ko FWY (2009) Application of quantified risk analysis in landslide risk management practice: Hong Kong experience. Georisk: Assess Manag Risk Engineered Syst Geohazards 3(3):134–146

Hungr O (1997) Some methods of landslide intensity mapping. In D.M. Cruden and R. Fell (eds.), Landslide risk assessment. Proceedings of the International Workshop on Landslide Risk Assessment, Honolulu, 19-21 February 1997. Balkema, Rotterdam: 215–226

Hungr O, Fell R, Couture R (eds.) (2005): Landslide risk management. Proceedings of the International Conference on Landslide Risk Management, Vancouver, 31 May – 3 June 2005. Taylor and Francis, London, pp 776

International Society of Soil Mechanics and Geotechnical Engineering – Technical Committee 304 (2004) http://jyching.twbbs.org/issmge/2004Glossary_Draft1.pdf

Jaiswal P, van Westen CJ, Jetten V (2010) Quantitative assessment of direct and indirect landslide risk along transportation lines in southern India. Nat Hazards Earth Syst Sci 10:1253–1267

Jaiswal P, van Westen CJ, Jetten V (2011) Quantitative estimation of landslide risk from rapid debris slides on natural slopes in the Nilgiri hills. India Nat Hazards Earth Syst Sci 11:1723–1743

Kaynia A, Papathoma-Köhle M, Neuhaeuser B, Ratzinger K, Wenzel H, Medina-Cetina Z (2008) Probabilistic assessment of vulnerability to landslide: application to the village of Lichtenstein, Baden-Württemberg, Germany. Eng Geol 101(1–2):33–48

Lee EM, Jones DKC (2013) Landslide risk assessment (2nd ed.). ICE, London, p 428

Li Z, Nadim F, Huang H, Uzielli M, Lacasse S (2010) Quantitative vulnerability estimation for scenario-based landslide hazards. Landslides 7(2):125–134

Mansour MF, Morgenstern NR, Martin CD (2011) Expected damage from displacement of slow-moving slides. Landslides 8(1):117–131

Mavrouli O, Corominas J (2010) Vulnerability of simple reinforced concrete buildings to damage by rockfalls. Landslides 7(2):169–180

Ragozin AL, Tikhvinsky IO (2000) Landslide hazard, vulnerability and risk assessment. In: Bromhead E, Dixon N, Ibsen ML (eds) Proceedings of the 8th International Symposium on Landslides, Cardiff: 1257–1262

Sassa K, Canuti P (eds) (2008) Landslides—disaster risk reduction. Proceedings of the First World Landslide Forum. Springer, Berlin, p 650

Spence RJS, Kelman I, Calogero E, Toyos G, Baxter PJ, Komorowski JC (2005) Modelling expected physical impacts and human casualties from explosive volcanic eruptions. Nat Hazards Earth Syst Sci 5:1003–1015

UNDRO - United Nations Disaster Relief Organization (1979) Natural disasters and vulnerability analysis. Geneva, pp 53

Uzielli M, Catani F, Tofani V, Casagli N (2014) Risk analysis for the Ancona landslide—I: characterization of landslide kinematics. Submitted as companion paper. doi:10.1007/s10346-014-0474-0

Uzielli M, Nadim F, Lacasse S, Kaynia AM (2008) A conceptual framework for quantitative estimation of physical vulnerability to landslides. Eng Geol 102:251–256

Zêzere JL, Garcia RAC, Oliveira SC, Reis E (2008) Probabilistic landslide risk analysis considering direct costs in the area north of Lisbon (Portugal). Geomorphology 94:467–495

M. Uzielli (✉)
Georisk Engineering S.r.l.,
Florence, Italy
e-mail: muz@georisk.eu

F. Catani · V. Tofani · N. Casagli
Department of Earth Sciences,
University of Florence,
Florence, Italy